IEEE/CSC & ESAS European Superconductivity News Forum (ESNF), No. 6, October 2008
(ASC Preprint 5LX07 conforming to IEEE Policy on Electronic Dissemination, Section 8.1.9)

The published version of this manuscript appeared in *IEEE Transactions on Applied Superconductivity* **19**, No. 3, Part 2, 1235 - 1239 (2009)

Design of HQ – a High Field Large Bore Nb_3Sn Quadrupole Magnet for LARP

H. Felice, G. Ambrosio, M. Anerella, R. Bossert, S. Caspi, D. Cheng, D. Dietderich, P. Ferracin, A. K. Ghosh, R. Hafalia, C. R. Hannaford, V. Kashikhin, J. Schmalze, S. Prestemon, G.L. Sabbi, P.Wanderer, A.V. Zlobin

***Abstract*— In support of the Large Hadron Collider luminosity upgrade, a large bore (120 mm) Nb_3Sn quadrupole with 15 T peak coil field is being developed within the framework of the US LHC Accelerator Research Program (LARP). The 2-layer design with a 15 mm wide cable is aimed at pre-stress control, alignment and field quality while exploring the magnet performance limits in terms of gradient, forces and stresses. In addition, HQ will determine the magnetic, mechanical, and thermal margins of Nb_3Sn technology with respect to the requirements of the luminosity upgrade at the LHC.**

***Index Terms*— Superconducting accelerator magnets, Nb_3Sn, IR quadrupole, LARP**

I. INTRODUCTION

UPGRADING the LHC baseline luminosity requires IR quadrupoles with large aperture and high gradients. The main objective of LARP is to demonstrate the feasibility of Nb_3Sn technology for the LHC Phase 2 upgrade. Toward this goal, LARP has developed several series of Nb_3Sn magnets: the SQ series (Subscale Quadrupole) [1], [2], the TQ series (1-meter long 90 mm aperture Technology Quadrupole) [3], [4] and the LRS series (3.6-meter Long Racetrack assembled in a common coil arrangement) [5]. The LQ series (Long Quadrupole) is under construction and is a 3.7 long version of the TQ series aiming at demonstrating the scalability of Nb_3Sn cosine two theta quadrupole [6].

In order to meet the requirements for Phase 2 LHC upgrade, the next series of magnet will have to be designed to reach 15 T at 1.9 K in a large aperture (above 110 mm) with alignment features (to provide field quality), cooling channels and LHe containment. The objective of the LARP HQ series (1-meter long High gradient, high field Quadrupole) is to address these requirements.

With the Phase 1 LHC upgrade, CERN is going to fabricate IR quadrupole magnets using NbTi. This intermediate LHC upgrade and the ongoing development on HQ give a good opportunity to compare the performances of NbTi and Nb_3Sn large aperture quads. In order to match the CERN NbTi quads aperture, the aperture of HQ will be 120 mm [7], [8]. The 2D magnetic design along with some preliminary results on the 3D magnetic design is summarized in this paper. In the last part, the mechanical structure implementing alignment features is presented.

Manuscript received 26 August 2008. This work was supported in part by the Director, Office of Energy Research, Office of High Energy and Nuclear Physics, High Energy Physics Division, U.S. Department of Energy, under contract No. DE-AC02-05CH11231.

H.Felice, S. Caspi, D. Dietderich, D. Cheng, P. Ferracin, R. Hafalia, C.R. Hannaford, S. Prestemon and GL Sabbi are with Lawrence Berkeley National Laboratory, Berkeley, CA 94720 USA (e-mail: HFelice@lbl.gov).

G. Ambrosio, R. Bossert, V. Kashiskhin and A.Zlobin are with Fermilab National Accelerator Laboratory, Batatvia, IL 60510-0500 USA.

M. Anerella, A. K. Ghosh, J. Schmalze and P. Wanderer are with Brookhaven National Laboratory, NY, USA

II. MAGNETIC DESIGN

A. Conductor

The objectives of HQ are to reach 15 T peak field in the conductor and 200 T/m in a 120 mm aperture. A wide cable was selected to achieve this goal in a 2-layer cos2θ quadrupole and to manage the mechanical stresses in the coil. In addition, CERN plans to use the 15.1 mm wide LHC main dipole cable to fabricate the Phase 1 IR NbTi quadrupole magnets [9], [10]. In order to facilitate the comparison between NbTi and Nb_3Sn quads, the cable width of HQ was chosen to match that of the dipole cable, 15.15 mm. The present conductor parameters are described in Table I. Due to the large size of the cable and its keystone angle, prototype cables were fabricated. The cables have been evaluated for their windability and if any strand damage occurred during cabling.

TABLE I HQ DESIGN PARAMETERS

Parameters	Units	HQ design
Strand diameter	mm	0.8 +/- 0.003
Strand type		OST RRP 54/61 [11]
Cu/non-Cu ratio		0.87
Number strands		35
Cable width (bare)	mm	15.15 +/- 0.025
Cable mid-thickness (bare)	mm	1.437 +/- 0.010
Keystone angle	deg	0.75 +/- 0.05
Insulation thickness	μm	100
Nb of turns IL/OL		20/25

Several prototype cables have been fabricated with different thickness and keystone angles and each cable's behavior was characterized by winding tests around various pole

geometries. The fabrication of the pole pieces used Stereolithography (SLA), a Rapid Prototyping (RP) technique, for quick part turnaround with minimal tooling costs. The SLA process uses a laser to cure photosensitive resin in thin (127 micrometers) layers that are essentially cross-sectional slices of virtually any three-dimensional shape.

The rating of these prototype cables allowed us to converge on the cable dimension reported in Table I. These numbers are part of an optimization process and are still underway. Let's note that the cable mid-thickness used in the cross-section design is equal to 1.43 mm and the insulation thickness is equal to 0.11 mm.

B. Reference Cross-section

The experience on TQ and LQ illustrated the importance of combining the magnetic design with the mechanical design. It has been shown in [12] and [13] that the optimization of components surrounding the coil in the LQ shell structure improved the stress distribution in the outer layer of the coil. Nevertheless, the LQ outer layer remains overloaded, exhibiting 85 MPa of compression at the pole/coil contact in the outer layer when the inner layer is fully unloaded. This stress distribution is due to the imbalance of the azimuthal Lorentz forces distribution between the two layers: -1.5 MN/m in the inner layer and –1 MN/m in the outer layer.

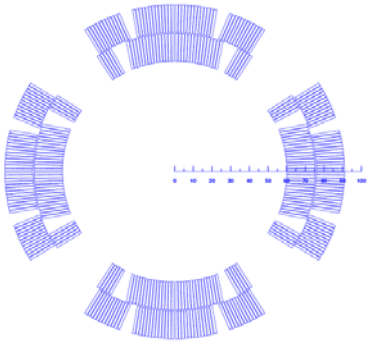

Fig 1. HQ magnetic cross-section

TABLE II 2D MAGNET PARAMETERS AT SHORT SAMPLE*

Parameters	Units	4.2 K	1.9 K
Gradient	T/m	202.6	219.3
Current	kA	18.3	19.9
Coil peak field	T	14.1	15.2
Inductance	mH/m	7.1	7.1
Stored Energy	MJ/m	1.2	1.4
X Lorentz force / octant	MN/m	2.9	3.4
Y Lorentz force / octant	MN/m	-4.2	-5
θ Lorentz force IL/OL	MN/m	-2.1/-2.6	-2.5/-3.1

* Jc (4.2 K, 12 T) = 3000 A/mm^2

However, with the same azimuthal Lorentz forces in both layers, the outer layer will still exhibit some overloading. This is caused by the mechanical structure and is unavoidable to preload the inner layer. The only way to mitigate this behavior is to optimize the magnetic cross-section to obtain an azimuthal force higher in the outer layer than in the inner layer. The magnet parameters at short sample are presented in Table II and the optimized cross-section is represented in Fig. 1. The mid-plane shim is equal to 0.195 mm.

The NbTi Phase 1 quads are designed to operate at 120 T/m. For comparison, the HQ parameters at this operating gradient are summarized in Table III.

TABLE III MAGNET PARAMETERS AT OPERATING POINT

Parameters	Units	G_{op} = 120 T/m
Current	kA	10.5
% load line @ 4.2K	%	57
% loadline @ 1.9K	%	52
X Lorentz force / octant	MN/m	1.1
Y Lorentz force / octant	MN/m	-1.4
θ Lorentz force IL/OL	MN/m	-0.7/-0.9

In the cross-section shown in Fig. 1, the minimum pole width is 23.46 mm. Up to now, the winding tests have been performed on pole pieces as narrow as 22.57 mm giving a acceptable mechanical stability for some prototype cables. Consequently, this cross-section does not show any limitation in terms of windability.

C. Field quality

As described in part III, the mechanical structure presently considered for HQ is a shell-based structure. The iron pad and yoke shapes have been taken into account in the cross-section optimization in order to minimize the harmonics variation due to iron saturation. The shape and material of the mechanical parts are essential for the mechanical behavior of the structure. Therefore, the mechanical analysis and the yoke design have been conducted in parallel.

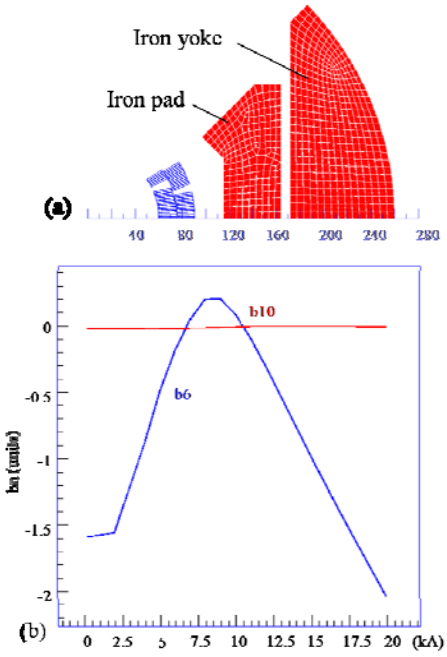

Fig. 2. (a) Octant of the iron yoke and pad cross-section – (b) Variation of b6 and b10 in units versus the HQ current

The cross-section of the iron yoke and pad is presented in Fig. 2-(a). The mid-plane distance between the pad and the coil is equal to 24 mm and the shape of the pad has been improved to reduce the b_6 variation induced by the saturation. The reference radius is taken at 40 mm. For a gradient between 0 and 120 T/m (10.5 kA), the variation of b_6 ranges between –1.6 and 0.25 units, while b_{10} is constant and equal to 0.005 units. The persistent current effects have not yet been taken into account but could be corrected with some iron shimming strategy as proposed in [14].

D. 3D Analysis

Some preliminary 3D computations have been performed in order to check that the iron shape, compatible from a saturation stand point, allowed also to obtain the peak field in the straight section of the coil. The first results show that whatever the arrangement of the coil ends, if the yoke and pads are full length, the peak field is 2 to 4 % higher in the coil ends. On the contrary, as illustrated in Fig. 3, if the yoke and pads are shortened and the inner layer pole piece longer than the outer layer pole piece, the peak field can be 3% lower in the ends than in the straight section. This difference goes down to 2 % if the yoke is full length and the pads short. These preliminary results show that the iron yoke and pads shape allow keeping the coil peak field in the straight section while minimizing the impact on the harmonics.

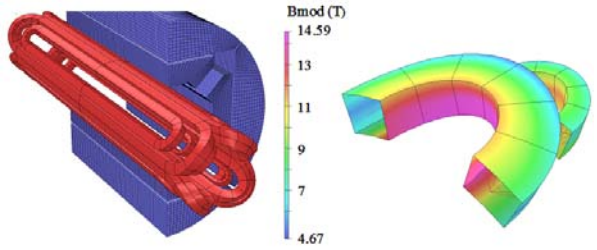

Fig. 3. 3D preliminary results – B_{end} = 14.59 T and $B_{straight}$ = 15.03 T with inner layer pole longer than outer layer pole

III. 2D Mechanical Design

A. Mechanical Structure

In order to provide the large force required to preload HQ without risking any overstress during assembly, the mechanical structure considered presently is a shell-based structure [15]. In this last design, less than 40 % of the preload is provided at room temperature by the bladder and key operation. The main part of the pre-stress is achieved during cool-down by the shrinkage of the outer aluminum shell.

A cross-section and an exploded view of the mechanical structure are shown in Fig. 4 and 5. The coils are wound around titanium-alloy poles. With respect to the LQS structure, an aluminum bolted collar has been introduced between the coil and the pad aiming at aligning the coil with the structure. This collar is made of four 90 degrees pieces bolted against a stainless steel pole key pinned in the titanium pole of the coil. This aluminum collar is 24 mm thick on the mid-plane to satisfy the suitable distance between coil and iron. The LQS structure uses two so-called master keys (one on the pad side, one on the yoke side) to facilitate the assembly procedure of a 3.7-meter long magnet. In addition to this assembly purpose, the master keys are also used to maintain alignment between the pad and the yoke since they are “forced” in place during the bladder operation.

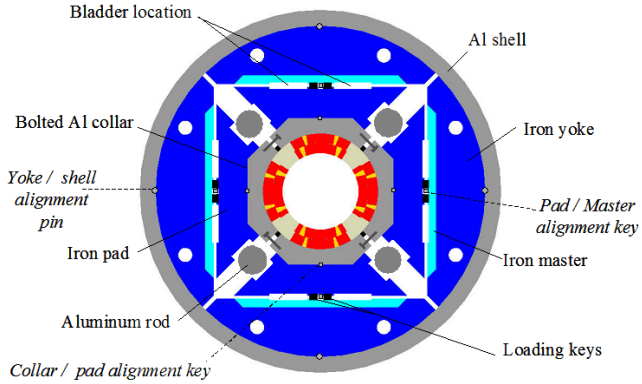

Fig. 4. Cross-section of the mechanical structure

In the 1-meter long HQ case, the assembly of the magnet is not a primary concern and a single master key can be used on the yoke side to provide the alignment between the pad and the yoke.

The aluminum shell is 25 mm thick; the outer radius of the yoke is equal to 260 mm. Some empty space has been provided at 45 degrees for cooling channels. Two nominal loading keys are positioned at 5 mm from the mid-plane. Some cut outs are introduced in the pad in order to provide room for the aluminum axial rods. Alignment keys are introduced on the mid-plane between the bolted collar and the iron pad and between the iron pad and the yoke master key. Similarly to LQS, alignment pins are used between the yoke and the shell [13].

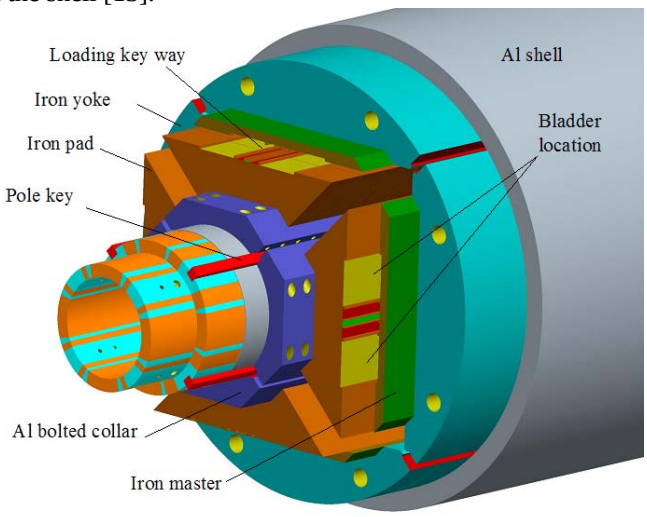

Fig. 5. Exploded view of the mechanical structure showing dummy coils.

B. Mechanical analysis

One octant of HQ has been analyzed in 2D with ANSYS. Bladder operation, loading key insertion, cool-down and excitation have been simulated in the 4.2 K and 1.9 K short sample conditions with a friction coefficient of 0.2. All the contact elements between the components allow sliding and separation except the contact element between the two double-layer and the pole/coil contacts, which are glued. Therefore, a

lack of preload results in a tensile stress at the pole-coil contact when e.m. forces are applied. In order to reduce the azimuthal stress in the winding, the epoxy is assumed to withstand a maximum tension of 20 MPa at the short sample limit. Regarding the boundary conditions, zero displacement is imposed on the mid-plane and at 45° to the pole, to the pole key and to the shell.

In order to provide alignment, the aluminum collar has to remain in compression with the pole key from the bladder operation to the excitation of the magnet. The FE analysis shows that it is the case since the collar remains in contact with the pole key at each step. The introduction of the bolted collar intercepts 20 % of the preload provided by the bladder operation and the cool-down. The amount of preload intercepted depends mainly on the engagement of the pole key in the collar, which is 1 cm long in the model.

The results of the analysis are shown in Table IV. The preload gradient column indicates the maximum gradient considered for the magnet preload. For the short sample conditions at 1.9 K and 4.2 K, the preload gradient is equal to the short sample gradient. For a lower operating point, like 120 T/m, the preload gradient would have to be higher and could be of the order of 150 T/m. In the short sample condition at 1.9 K and 4.2 K, the bladder operation is performed with 60 mm bladders pressurized at 38 MPa in order to open a clearance large enough for the shimming of the load keys. During this operation, the peak stress in the coil remains safely below 90 MPa. The maximum stress in the coil occurs after cool down with a peak stress in the upper block of the inner layer. To reduce this peak stress, a release cut in the pole could be considered.

TABLE IV MECHANICAL ANALYSIS

Parameters	Units	4.2 K	1.9 K
Preload Gradient	T/m	202.6	219.3
Bladder pressure	MPa	35	38
COIL			
Pole/coil contact	MPa	-5	+20
$\sigma_{\theta\ max}$ bladder	MPa	-84	-90
$\sigma_{\theta\ max}$ loading key	MPa	-75	-82
$\sigma_{\theta\ max}$ cool-down	MPa	-171	-177
$\sigma_{\theta\ max}$ Lorentz	MPa	-151	-171
SHELL			
$\sigma_{\theta\ max}$ loading keys	MPa	160	175
$\sigma_{\theta\ max}$ cool-down	MPa	251	266
YOKE MASTER			
$\sigma_{1\ max}$ Lorentz	MPa	127	134
YOKE			
$\sigma_{1\ max}$ Lorentz	MPa	152	161

[a] Bladder size 40 mm
[b] Shell thickness 18 mm

Although the azimuthal stress $\sigma_{\theta\ max}$ reached at 1.9 K with Lorentz forces is well above the degradation limit of 150 MPa currently assumed for the Nb_3Sn conductor, it might be tolerated because it occurs in a region where the field is ~1.5 T lower than the peak field. For gradients below 170 T/m, the stresses induced in the winding are below 150 MPa.

In all cases, all the iron parts exhibit first principal stresses below 160 MPa and the azimuthal stress in the shell remains below 270 MPa ensuring the integrity of all the structural parts.

C. LHe containment

Because of the shell-based concept, an additional external cylinder must be considered for the LHe containment. An option is to weld a stainless steel skin around the aluminum shell. This additional shell does not impact the behavior of the structure. It is important to keep in mind that even if most of the preload is provided by the shrinkage of the aluminum shell, the overall shrinkage of the structure is driven by the iron yoke and pads thermal contraction which is of the order of 1.97 mm/m from 300 K to 4.2 K. Therefore, a welded stainless steel shell, whose thermal contraction is ~ 2.8 mm/m, should remain in contact with the aluminum shell. Preliminary computations have been made and show that if the stainless steel shell is welded with a tension of 80 MPa, the increase of stress in the coil is of the order of 10 MPa, which could be taken into account during assembly.

Another option is the possibility to insert the magnet directly in an external stainless steel tube: this choice would eliminate the welding stage.

IV. CONCLUSION

The HQ 2D magnetic cross-section and iron yoke and pad have been designed to achieve a good field quality and to position the peak field in the straight section of the magnet. The magnetic design is closely linked to the mechanical design. The mechanical structure implementing alignment can provide support to the coil up to the 1.9 K short sample limit of the magnet with an acceptable mechanical stress level in the coil. Some optimizations are still in progress.

REFERENCES

[1] P. Ferracin *et al.*, "Development of Large Aperture Nb3Sn Racetrack Quadrupole Magnet," *IEEE Trans. Appl. Supercond.*, vol. 15, Issue 2, June 2005.

[2] P. Ferracin *et al.*, "Assembly and Tests of SQ02, a Nb_3Sn Racetrack Quadrupole Magnet for LARP", *IEEE Trans. Appl. Supercond.*, vol. 17, Issue 2, June 2007.

[3] S. Caspi *et al.*, "Test Results of LARP Nb3Sn Quadrupole Magnets Using a Shell-based Support Structure (TQS)", presented at ASC 2008, 17-22 August 2008, Chicago, IL, USA.

[4] R. Bossert *et al.*, "Fabrication and Test of LARP Technological Quadrupole Models of TQC series", presented at ASC 2008, 17-22 August 2008, Chicago, IL, USA.

[5] P. Wanderer et al., "Construction and Test of 3.6 m Nb_3Sn Racetrack Coils for LARP," *IEEE Trans. Appl. Supercond.*, Vol. 18, No 2, June 2008.

[6] G. Ambrosio *et al.*, "Development of LARP 3.7 m Long Nb3Sn Quadrupole Models", presented at ASC 2008, 17-22 August 2008, Chicago, IL, USA.

[7] R. Ostojic, "LHC Interaction Region Upgrade – Phase I, "LHC PR 1094, August 2008, http://cdsweb.cern.ch/record/1119948/files/LHC-PROJECT-REPORT-1094.pdf

[8] J.P. Koutchouk, L. Rossi and E. Todesco, "A solution for Phase-one Upgrade of the LHC Low-beta Quadrupoles based on NbTi", LHC PR

1000, http://cdsweb.cern.ch/record/1027327/files/note-2007-006-HHH.pdf

[9] CERN, LHC Design Report, vol.1, The LHC Main Ring, , June 2004, http://ab-div.web.cern.ch/ab-div/Publications/LHC-DesignReport.html

[10] F. Borgnolutti *et al*., "130 mm aperture Quadrupoles for the LHC Luminosity Upgrade," *Proceedings of PAC07*, June 2007, http://accelconf.web.cern.ch/accelconf/JACoW/proceedingsnew.htm

[11] J. A. Parell *et al*., "High Field Nb_3Sn Conductor Development at Oxford Superconducting Technology," *IEEE Trans. Appl. Supercond*., Vol. 13, No , June 2003.

[12] H. Felice, "Nb_3Sn Quadrupole Designs for the LHC Upgrade", presented at WAMSDO 2008, CERN, Switzerland, 19-23 May 2008, http://indico.cern.ch/conferenceDisplay.py?confId=28832

[13] P. Ferracin *et al*., "Fabrication and Test of a 3.7 m Long Support Structure for the LARP Nb3Sn Quadrupole Magnet LQS01", presented at ASC 2008, 17-22 August 2008, Chicago, IL, USA.

[14] V. V. Kashikhin *et al.*, "Passive Coreection of the Persistent Current Effect in Nb_3Sn Accelerator Magnets," *IEEE Trans. Appl. Supercond*., Vol. 18, No 2, June 2008.

[15] H. Felice et al., "Magnetic and Mechanical Analysis of the HQ Model Quadrupole Designs for LARP," *IEEE Trans. Appl. Supercond.*, Vol. 18, No 2, June 2008.